IEEE Access
Multidisciplinary ⋮ Rapid Review ⋮ Open Access Journal

Received April 4, 2022, accepted April 15, 2022, date of publication April 20, 2022, date of current version April 28, 2022.

Digital Object Identifier 10.1109/ACCESS.2022.3169012

Event-Triggered Adaptive Neural Tracking Control of Flexible-Joint Robot Systems With Input Saturation

XINGLEI XU AND SHIWEI XU
School of Artificial Intelligence, Wenzhou Polytechnic, Wenzhou, Zhejiang 325035, China
Corresponding authors: Xinglei Xu (xuxinglei2022@sina.com) and Shiwei Xu (xingleixu@wzpt.edu.cn)

ABSTRACT This paper investigates an event-triggered adaptive neural tracking control issue for flexible-joint robot (FJR) systems subject to unknown dynamic and input saturation. To enable the backstepping design framework to be implemented, the input saturation nonlinearity is replaced by a smooth function. In the control design, the dynamic surface control (DSC) and adaptive neural techniques are used to handle the ''explosion of complexity'' issue and unknown dynamics, respectively. Furthermore, to reduce the calculated burden caused by the adaptive neural reconstruction technique, three virtual parameters are updated by using the single-parameter-learning approach. To decrease the frequency of actuator response to the control command for reducing the mechanical wear of actuator, an event triggering mechanism is established between the control law and actuator. Finally, an event-triggered adaptive neural tracking control solution is proposed, which is endowed the advantages as: (1) it does not need any *priori* knowledge of FJR systems; 2) it only needs to update three unknown parameters; 3) it can reduce the transmission frequency of the control commands and the response rate of the actuator. Using the Lyapunov stability theory, the proposed event-triggered control solution ensures that all signals of the closed-loop tracking control system are bounded. Finally, the simulation results verify the effectiveness and superiority of the proposed control scheme.

INDEX TERMS Flexible-joint robot, adaptive neural tracking control, event triggering control, input saturation, dynamic surface control.

I. INTRODUCTION

For the past few years, intense interests have been paid close attention to the modeling and control of flexible joint robot (FJR) systems [1]–[3], [5], [14] due to its important role in civil and military affairs. To solve the control issue of FJR systems, many effective control methods have been reported, such as uncertain observer [6], PID/PD control [7]–[9], adaptive sliding mode control [10], feedback linearisation control [11], [12], passivity control [13], singular perturbation control [14], adaptive backstepping control [15]–[17], *etc*. In practice, due to the modeling technique and plant's nonlinear character, the FJR systems inevitably suffer from the uncertainties. In this context, the difficulty of control design derives from the uncertain and nonlinear characteristic. For the control issue of uncertain nonlinear systems, the adaptive backstepping design framework reveals its unique advantage [18]. However, owing to the recursive design process, the virtual control function needs to be differentiated repeatedly such that there exists a drawback called the ''explosion of complexity'' in the design framework. To solve such a problem, Swaroop *et al.* [19] proposed the dynamic surface control (DSC) scheme for a class strict-feedback nonlinear systems, in which a first-order filter is introduced into the each step of the traditional backstepping design. Based on the DSC method, many significative research results have also been reported to solve the control issue of FJR systems [20]–[22].

To compensate the uncertainty of FJR systems, several effective approaches, such as extended state observer (ESO) [23]–[25], time-delay estimation [26], [27], neural network (NN) [28], [29], fuzzy logic system (FLS) [30], [31], *etc*. To avoid the problem of ''explosion of complexity'' in the works [29]–[31], Joo *et al.* [32] and Miao *et al.* [33] introduced a first-order filter into the backstepping design such that the differential operation of virtual control law is

The associate editor coordinating the review of this manuscript and approving it for publication was Bidyadhar Subudhi.

replaced by the algebraic operation. The other implicit benefit of such an operation is that the input dimensionality of NN or FLS is reduced greatly [34]. It should be pointed out that the works in [29]–[32] surfer from the dimensional curse issue [35]. To this end, for the control issue of FJR systems, Ling *et al.* [36] taken the minimum learning parameter technique [34] into the DSC design framework to solve the dimensional curse issue.

In practice, for any physical systems, input saturation is an inevitable problem, which ascribes the physical property of actuator. In the existing works, many effective methods have been reported to handle the input saturation issue, such as the domain of attraction [37], gain scheduling [38], model augmentation [39], auxiliary dynamic design [40], [41], smooth function substitution [42], *etc*. It should be pointed out that the method based on the domain of attraction requires the knowledge of plant; the gain scheduling-based method requires the mapping between system response performance and control gain, which leads to the closed-loop system incredibly complex; the model augmentation requires that the plant needs to be augmented with a first-order form, which increases the difficulty of control design. Compared with the model augmentation, the auxiliary dynamic design can simplify the control design, but it may introduce a non-smooth signal into the closed-loop system. For such an issue, a smooth function is used to replace the non-smooth saturation nonlinearity in the smooth function substitution-based method [36]. Nevertheless, the work [36] required the part model knowledge, which leads to the control solution difficulty to be implemented. Furthermore, Ding *et al.* [43] employed the neural approximation technique to reconstruct the unknown dynamic of FJR systems with input saturation.

Although the above methods effectively have solved the problems of unknown system dynamic, a practical problem, i.e., the actuator has a working range in the command response frequency, is not considered. In addition, owing to the sensor measurement noise, the high-frequency noise may enter into the closed-loop system, which leads to the high frequency response of the actuator and mechanical wear of actuator. Therefore, it is essential how to reduce the mechanical wear of actuator to achieve the purpose of reducing the frequency of actuator failures. For such an issue, the event-triggered control (ETC) [44], [45] method has its preponderance, in which the control commands are transmitted only if a certain event is triggered [46]–[49]. Based on this idea, the event-triggered control for FJR systems has attracted the attention of many scholars [50], [51]. In [52], an event-triggered adaptive asymptotically tracking control solution for a single-Link Robot was proposed, in which the transmitting and computation burdens of control commands are effectively reduced by using the DSC and ETC techniques. It is should be pointed out that the event triggering mechanisms proposed in [50]–[52] only taken the measuring error of control input into account, but the control accuracy was not considered in the design. However, for the FJR systems, the control accuracy also needs to be followed in the design of event triggering mechanism.

Motivated by the previous works, an event-triggered adaptive neural tracking control scheme for FJR systems under unknown dynamics and input saturation is presented. The main contributions can be summarized as follows.

- This work proposed a DSC-based adaptive neural tracking control scheme, in which a single parameter learning and adaptive neural network techniques are used to handle the unknown dynamics and parameters. Compared with the work [29], [31], [32], our proposed control solution does not require any *priori* knowledge of plant.
- Different from the event triggering mechanism [50]–[52], the event triggering mechanism proposed in this work includes the internal and external trigger condition. As a result, the transmission frequency of the control commands and the execution rate of the actuator not only are drastically reduced, but also the control performance can be ensured.
- Using the single-parameter-learning idea, this work designs three adaptive laws and each one requires only one regressor, which avoids the problem of dimensional curse in [29]–[31], and overcomes the design difficulty caused by the unknown gains of FJR systems.

The rest of this paper is arranged as follows. In Section 2, the mathematical model of MSVs and the problem formulation are introduced. In Section 3, the principle of intelligent approximation using NN is presented. In Section 4, proposes the details of controller design procedures. In Section 5, the simulation results are given to show the effectiveness of the controller. In Section 6, the entire work is summarized.

II. PROBLEM FORMULATION AND PRELIMINARIES

A. PROBLEM FORMULATION

According to the Euler-Lagrangian (EL) equation, the single-link FJR dynamics can be described as follows [36]

$$\mathcal{M}\mathcal{L}^2\ddot{q} + \mathcal{M}g\mathcal{L}\sin(q) + \mathcal{F}(\dot{q}) + \mathcal{K}q = \mathcal{K}q_m \tag{1}$$

$$\mathcal{J}\ddot{q}_m + \mathcal{B}\dot{q}_m + \mathcal{K}(q - q_m) = u \tag{2}$$

where q, $\dot{q}$ and $\ddot{q}$ denote the link position, velocity, and acceleration of FJR, respectively. q_m, $\dot{q}_m$ and $\ddot{q}_m$ denote the rotor angular position, velocity, and acceleration, respectively. $\mathcal{M}$, $\mathcal{L}$ and g denote the mass and length of link and the gravity acceleration, respectively. $\mathcal{F}(\dot{q})$ is the friction. $\mathcal{K}$, $\mathcal{J}$ and $\mathcal{B}$ denote the coefficients of joint stiffness, the joint flexibility and the damping, respectively. u is the actual control input of plant.

Considering the issue of actuator's physical constraint, the control input u is subjected to input saturation, which can be described by

$$u = \begin{cases} \text{sgn}\,(u_c)\,|u_m|, & |u_c| > u_m \\ u_c, & |u_c| \le u_m \end{cases} \tag{3}$$

where u_c is the control command generated by control law, sgn$(\cdot)$ denotes the sign function, and u_m is the maximum value of actuator control input.

Considering the issue of actuator's physical constraint, the control input u is subjected to input saturation, which can be described by

$$u = \begin{cases} \text{sgn}\,(u_c)\,|u_m|, & |u_c| > u_m \\ u_c, & |u_c| \le u_m \end{cases} \tag{4}$$

where sgn$(\cdot)$ denotes the sign function, and u_m is the maximum value of actuator control input.

Remark 1: In practice, due to the modeling technique, nonlinear characteristic, etc., it is very difficult to obtain the accurate knowledge of the model parameters of FJR systems. In addition, the friction $\mathcal{F}(\dot{q})$ is not modelable. For the tracking control issue, it is common that the reference trajectory y_d and its derivatives $\dot{y}_d$ and $\ddot{y}_d$ are required to known. Similar requirements are also mentioned in [2], [32], [33], [36]. Therefore, assumptions 1-2 are reasonable.

According to (4), the u is a non-smooth function with respect to u_c. To facilitate the implementation of backstepping design framework, a smooth function is used to replace the non-smooth nonlinear function u, i.e.,

$$u(u_c) = u_m \mathcal{G}\left(\frac{\sqrt{\pi}u_c}{2u_m}\right) \tag{5}$$

where $\mathcal{G}(\cdot)$ is the Gaussian error function defined as $\mathcal{G}(\nu) = \frac{2}{\sqrt{\pi}}\int_0^{\nu} e^{-t^2}dt$. Here, $u(u_c)$ is written as

$$u(u_c) = \delta(u_c) + d(u_c) \tag{6}$$

where $d(u_c)$ is the approximate error, which satisfies $|d(u_c)| = |u(u_c) - \delta(u_c)| \le D$ with D being a positive constant.

According to Mean-value theorem, $\delta(u_c)$ can be written as

$$\delta(u_c) = \delta(0) + \epsilon\tau_c \tag{7}$$

where $\epsilon = \exp\left(-\left(\frac{\sqrt{\pi}\iota u_c}{2u_m}\right)^2\right)$, $0 < \iota < 1$, i.e., there exist a constant ω satisfying $0 < \omega < \epsilon$. Furthermore, using (5)-(7), one can get

$$u(u_c) = \epsilon\tau_c + d(u_c) \tag{8}$$

Let $x_1 = q$, $x_2 = \dot{q}$, $x_3 = q_m$ and $x_4 = \dot{q}_m$, and using (8), we have

$$\begin{cases} \dot{x}_1 = x_2 \\ \dot{x}_2 = \psi_1 x_3 + f_2(\bar{\boldsymbol{x}}_{\boldsymbol{2}}) \\ \dot{x}_3 = x_4 \\ \dot{x}_4 = \psi_2\epsilon u + f_4(\bar{\boldsymbol{x}}_{\boldsymbol{4}}) + d \end{cases} \tag{9}$$

where $\psi_1 = \mathcal{K}/\mathcal{ML}_2$, $\psi_2 = \mathcal{J}^{-1}$, $f_2(\bar{\boldsymbol{x}}_{\boldsymbol{2}}) = -\frac{\mathcal{K}x_1 + \mathcal{F}(x_2)}{\mathcal{ML}^2} - \frac{g\sin x_1}{L}$, $f_4(\bar{\boldsymbol{x}}_{\boldsymbol{4}}) = -\mathcal{J}^{-1}(\mathcal{B}x_4 + \mathcal{K}(x_3 - x_1))$ and $d = \psi_2 d(u_c)$. From $|d(u_c)| \le D$, there exists a constant ψ_d satisfying $|d| \le \psi_d$. In addition, according to $0 < \omega < \epsilon$ and $\epsilon \in (0, 1]$, there exists a constant ψ_ϵ such that $\psi_2\epsilon \ge \psi_\epsilon$ can be held.

Remark 2: From Assumption 1, we know that $\psi_i, i = 1, 2$, is unknown, and $f_2(\bar{\boldsymbol{x}}_{\boldsymbol{2}})$ and $f_4(\bar{\boldsymbol{x}}_{\boldsymbol{4}})$ are unknown function. Nonlinear function $f_2(\bar{\boldsymbol{x}}_{\boldsymbol{2}})$ contains $\mathcal{F}(\dot{q})$, which is unmodelable. Thus, $f_2(\bar{\boldsymbol{x}}_{\boldsymbol{2}})$ can not be linearly parameterized. In order to handle the problem, we will utilize RBF NNs to approximate the unknown nonlinear function $f_2(\bar{\boldsymbol{x}}_{\boldsymbol{2}})$ and $f_4(\bar{\boldsymbol{x}}_{\boldsymbol{4}})$.

The control objective of this paper is to design an event-triggered adaptive NN control law u_c for the single-link FJR system (1)-(2) under Assumptions 1-2 such that the actual trajectory y tracks a reference trajectory y_d, while ensuring that all signals in the closed-loop single-link FJR control system are bounded.

B. PRELIMINARIES

Lemma 1 ([40]): Any nonlinear function $\beta(\boldsymbol{X}) : R^n \to R$ defined on a compact set $\Omega_X \in R^n$ can be estimated by the radial basis function (RBF) NN $\boldsymbol{\xi}^{*T}\boldsymbol{\Psi}(\boldsymbol{X})$, and then we have

$$\beta(\boldsymbol{X}) = \boldsymbol{\xi}^{*T}\boldsymbol{\Psi}(\boldsymbol{X}) + \varepsilon \tag{10}$$

where the approximate error ε satisfies $|\varepsilon| \le \bar{\varepsilon}^*$ with $\bar{\varepsilon}^*$ being a positive constant. Vector $\boldsymbol{\xi}(\boldsymbol{X})$ represents the basis function. The ideal weight vector of NN is expressed as $\boldsymbol{\Psi}^* = [\Psi_1^*, \cdots, \Psi_\ell^*] \in R^l$. $\ell > 1$ is the number of node. The basis function $\boldsymbol{\xi}_i(\boldsymbol{X})$ is the Gaussian error function, that is,

$$\boldsymbol{\xi}_i(\boldsymbol{X}) = \exp\left[\frac{-(\boldsymbol{X} - \boldsymbol{c}_i)^T(\boldsymbol{X} - \boldsymbol{c}_i)}{\omega^2}\right] \tag{11}$$

where $\boldsymbol{c}_i = [c_{i1}, \cdots, c_{i\ell}]^T$ represents the center of the receptive area, and ω is the breadth of Gaussian function.

Lemma 2: Let $\bar{a}$ and $\bar{b}$ be scalars as well as $\flat$, m and n be positive constants. if $m > 1, n > 1$ and $(m-1)(n-1) = 1$ are held, there is

$$\bar{a}\bar{b} \le \frac{\flat^m}{m}|\bar{a}|^m + \frac{1}{\flat^m n}|\bar{b}|^n \tag{12}$$

III. MAIN RESULTS

In this section, we attempt to design an event-triggered adaptive neural tracking control (ETABTC) law using DSC design framework for the single-link FJR system. The design of ETABTC is based on the following change of coordinates:

$$z_1 = x_1 - y_d \tag{13}$$

$$z_i = x_i - \chi_i, \quad i = 2, 3, 4 \tag{14}$$

where χ_i is the filter version of the virtual control law α_{i-1}, which is produced by the following filter

$$\tau\dot{\chi}_i + \chi_i = \alpha_{i-1} \tag{15}$$

where $\chi_i \in R$ is the state of filter (15), and τ is the filter design constant. The filter initial conditions satisfy $\chi_i(0) = \alpha_{i-1}(0)$.

A. ROBUST ADAPTIVE NEURAL TRACKING CONTROL LAW DESIGN

In this subsection, we present the design procedure of ETABTC law, and the whole design procedure contains 4 steps. At each step, the virtual/atual control laws

are designed. At the step 2 and 4, the RBF NNs are applied to approximate unknown dynamics $f_2(\bar{x}_2)$ and $f_4(\bar{x}_4)$, respectively.

Step 1: Taking the time derivative of z_1, and using (9) and (13), one can get

$$\begin{aligned}\dot{z}_1 &= x_2 - \dot{y}_d \\ &= z_2 + \chi_2 - \alpha_1 + \alpha_1 - \dot{y}_d\end{aligned} \tag{16}$$

Design the virtual control law $\alpha_1 \in R^3$ as follows

$$\alpha_1 = -k_1 z_1 + \dot{y}_d \tag{17}$$

where $\kappa_1 \in R$ is a positive definite design constant.

Let $\vartheta_1 = \chi_2 - \alpha_1$. Substituting ϑ_1, (17) into (16), one can get

$$\dot{z}_1 = z_2 + \vartheta_1 - k_1 z_1 \tag{18}$$

Consider the following Lyapunov function candidate

$$V_1 = \frac{1}{2} z_1^2 + \frac{1}{2}\vartheta_1^2 \tag{19}$$

Taking the time derivative of V_1, and using $\vartheta_1 = \chi_2 - \alpha_1$, one has

$$\dot{V}_1 = -k_1 z_1^2 + z_1 z_2 + z_1\vartheta_1 + \vartheta_1\dot{\vartheta}_1 \tag{20}$$

According to $\vartheta_1 = \chi_2 - \alpha_1$ and (15), one has

$$\dot{\vartheta}_1 = -\tau^{-1}\vartheta_1 - \dot{\alpha}_1 \tag{21}$$

From (17), $\dot{\alpha}_1 = -k_1(x_2 - \dot{y}_d) + \ddot{y}_d$. According to [19], [34], $\dot{\alpha}_1$ is of the maxima value, i.e., $|\dot{\alpha}_1| \leq \bar{m}_1$. Furthermore, substituting (21) into (20), one can get

$$\begin{aligned}\dot{V}_1 &= -k_1 z_1^2 + z_1 z_2 + z_1\vartheta_1 - \vartheta_1(\tau^{-1}\vartheta_1 + \dot{\alpha}_1) \\ &\leq -(k_1 - 1)z_1^2 + 0.5 z_2^2 - (\tau^{-1} - 1)\vartheta_1^2 + 0.5\bar{m}_1^2\end{aligned} \tag{22}$$

Step 2: According to (9) and (14), the time-derivative of z_2 is given by

$$\dot{z}_2 = \psi_1 x_3 + f_2(\bar{\boldsymbol{x}}_2) - \dot{\chi}_2 \tag{23}$$

In (23), $f_2(\bar{x}_2)$ is an unknown function, which can be approximated using the RBF NN $\boldsymbol{\xi}_2^{*T}\boldsymbol{\Psi}(\bar{\boldsymbol{x}}_2)$ according to lemma 1. Then, $f_2(\bar{\boldsymbol{x}}_2)$ can be written as

$$f_2(\bar{\boldsymbol{x}}_2) = \boldsymbol{\xi}_2^{*T}\boldsymbol{\Psi}(\bar{\boldsymbol{x}}_2) + \varepsilon_2 \tag{24}$$

where $\boldsymbol{\xi}_2^* \in R^\ell$ is the ideal constant weight vector, $\boldsymbol{\Psi}(\bar{\boldsymbol{x}}_2) \in R^\ell$ is the base function vector, $\varepsilon_2 \in R$ is the approximation error satisfying $|\varepsilon_2| \leq \delta_2$ with δ_2 being an unknown positive constant. Let $\vartheta_2 = \chi_3 - \alpha_2$. Invoking (24) and ϑ_2 into (23) and using (13), it yields

$$\begin{aligned}\dot{z}_2 &= \psi_1 x_3 + \boldsymbol{\xi}_2^{*T}\Psi(\bar{\boldsymbol{x}}_2) + \varepsilon_2 - \dot{\chi}_2 \\ &= \psi_1\Big(z_3 + \alpha_2 - \vartheta_2 + \psi_1^{-1}\boldsymbol{\xi}_2^{*T}\Psi(\bar{\boldsymbol{x}}_2) \\ &\quad + \psi_1^{-1}\varepsilon_2 - \psi_1^{-1}\dot{\chi}_2\Big)\end{aligned} \tag{25}$$

Let $\mathcal{L}_1 = -\vartheta_2 + \psi_1^{-1}\boldsymbol{\xi}_2^{*T}\Psi(\bar{\boldsymbol{x}}_2) + \psi_1^{-1}\varepsilon_2 - \psi_1^{-1}\dot{\chi}_2 + \psi_1^{-1}z_2^2$. According to assumption 1, the term $\mathcal{L}_1$ is unknown. Taking the following operation for $\mathcal{L}_1$

$$\begin{aligned}|\mathcal{L}_1| &\leq |\psi_1^{-1}\boldsymbol{\xi}_2^{*T}\Psi(\bar{\boldsymbol{x}}_2)| + |\psi_1^{-1}\varepsilon_2| + \psi_1^{-1}|\dot{\chi}_2 - z_2^2 - \vartheta_2| \\ &\leq \varrho_1\beta_1(\boldsymbol{\varsigma}_1)\end{aligned} \tag{26}$$

where $\varrho_1 = \max\{||\psi_1^{-1}\boldsymbol{\xi}_2^{*T}||, |\psi_1^{-1}\varepsilon_2|, |\psi_1^{-1}|\}$ and $\beta_1(\boldsymbol{\varsigma}_1) = ||\Psi(\bar{\boldsymbol{x}}_2)|| + |\dot{\chi}_2 - z_2^2 - \vartheta_2| + 1$, with $\boldsymbol{\varsigma}_1 = [\bar{x}_2^T, \dot{\chi}_2, z_2, \vartheta_2]^T$. Using (26), one can get

$$\dot{z}_2 = \psi_1\Big(z_3 + \alpha_2 + \mathcal{L}_1\Big) - z_2^2 \tag{27}$$

Design the virtual control law α_2 as

$$\alpha_2 = -k_2 z_2 - \sigma_1\hat{\varrho}_1 z_2\beta_1^2(\boldsymbol{\varsigma}_1) \tag{28}$$

with adaptive law

$$\dot{\hat{\varrho}}_1 = \sigma_1 z_2^2\beta_1^2(\boldsymbol{\varsigma}_1) - \mu_1\hat{\varrho}_1 \tag{29}$$

where k_2, σ_1 and μ_1 are positive design constants.

Remark 3: According to the neural approximation principle, as the number of node ℓ is large enough, the RBF NN can approximate the unknown nonlinear function $f_2(\bar{\boldsymbol{x}}_2)$ with arbitrary precision, i.e., the approximation error ε_2 can be arbitrarily small. In practice, since the unknown nonlinear function $f_2(\bar{\boldsymbol{x}}_2)$ can not be modeled and may not satisfy the parameterized decomposition conditions. Therefore, the RBF NN is employed to implement the parameterized decomposition.

Remark 4: From (25), the unknown constant ψ_1 brings great trouble to the control design. If the conventional design method is used, an adaptive law needs to be designed to obtain the estimation value $\hat{\psi}_1$. Otherwise, ψ_1 needs to be assumed to be known. In this work, the single-parameter-learning method is introduced such that the difficulty in the control design is overcome dexterously. It should be pointed out that the design in this work utilizes the sign of ψ_1 adequately. Just because of this, this work does not require any any *priori* knowledge of FJR systems.

Consider the following Lyapunov function candidate

$$V_2 = V_1 + \frac{1}{2}z_2^2 + \frac{1}{2\psi_1}(\varrho_1 - \psi_1\hat{\varrho}_1)^2 + \frac{1}{2}\vartheta_2^2 \tag{30}$$

Taking the time derivative of V_2, and using (28)-(29) and (27), one can have

$$\begin{aligned}\dot{V}_2 \leq \dot{V}_1 + z_2\psi_1(z_3 + \alpha_2) + z_2\mathcal{L}_1 - z_2^2 - (\varrho_1 - \psi_1\hat{\varrho}_1)\dot{\hat{\varrho}}_1 \\ + \vartheta_2\dot{\vartheta}_2\end{aligned} \tag{31}$$

From (26), the term $z_2\mathcal{L}_1$ in (31) can be rewritten as

$$z_2\mathcal{L}_1 \leq |z_2|\varrho_1\beta_1(\boldsymbol{\varsigma}_1) \leq \sigma_1\varrho_1 z_2^2\beta_1^2(\boldsymbol{\varsigma}_1) + \frac{\varrho_1}{4\sigma_1} \tag{32}$$

Similarly, $\dot{\vartheta}_2 = -\tau^{-1}\vartheta_2 - \dot{\alpha}_2$. Here, $\dot{\alpha}_2$ is a continuous function, which is of the maxima value, i.e.,$|\dot{\alpha}_2| \leq \bar{m}_2$ according to [19], [34]. Furthermore, one can get

$$\dot{V}_2 \leq \dot{V}_1 + z_2\psi_1(z_3 - k_2 z_2 - \hat{\varrho}_1 z_2\beta_1^2(\boldsymbol{\varsigma}_1)) + \psi_1\varrho_1 z_2^2\beta_1^2(\boldsymbol{\varsigma}_1)$$

$$-(\varrho_1-\psi_1\hat{\varrho}_1)(\sigma_1 z_2^2\beta_1^2(\varsigma_1)-\mu_1\hat{\varrho}_1)-z_2^2$$
$$-\vartheta_2(\tau^{-1}\vartheta_2+\dot{\alpha}_2)+\frac{\varrho_1}{4\psi_1} \tag{33}$$

Using (32) and Lemma 2, one can get

$$\dot{V}_2\le-(k_1-1)z_1^2-(\tau^{-1}-1)\sum_{i=1}^{2}\vartheta_i^2+z_2\psi_1 z_3-\psi_1 k_2 z_2^2$$
$$+(\varrho_1-\psi_1\hat{\varrho}_1)\mu_1\hat{\varrho}_1+\frac{\varrho_1}{4\sigma_1}+\frac{2\bar{m}_1^2+\bar{m}_2^2}{4} \tag{34}$$

Furthermore, using Lemma 2, the term $(\varrho_1-\psi_1\hat{\varrho}_1)\hat{\varrho}_1$ can be rewritten as

$$(\varrho_1-\psi_1\hat{\varrho}_1)\hat{\varrho}_1\le-\frac{1}{2\psi_1}(\varrho_1-\psi_1\hat{\varrho}_1)^2+\frac{\varrho_1}{2\psi_1} \tag{35}$$

Substituting (35) into (34) yields

$$\dot{V}_2\le-(k_1-1)z_1^2-(\tau^{-1}-1)\sum_{i=1}^{2}\vartheta_i^2+z_2\psi_1 z_3-\psi_1 k_2 z_2^2$$
$$-\frac{\mu_1}{2\psi_1}(\varrho_1-\psi_1\hat{\varrho}_1)^2+\frac{\varrho_1\mu_1}{2\psi_1}+\frac{\varrho_1}{4\sigma_1}+\frac{2\bar{m}_1^2+\bar{m}_2^2}{4} \tag{36}$$

Step 3: Taking the time derivative of z_3, and using (9) and (14), one can get

$$\dot{z}_3=x_4-\dot{\chi}_3=z_4+\chi_4-\dot{\chi}_3 \tag{37}$$

Let $\vartheta_4=\chi_4-\alpha_3$. Then, consider the following Lyapunov function candidate

$$V_3^*=V_2+z_3^2 \tag{38}$$

Taking the time-derivative of V_3, and using (36) yields

$$\dot{V}_3^*\le-(k_1-1)z_1^2-(\tau^{-1}-1)\sum_{i=1}^{2}\vartheta_i^2-\psi_1 k_2 z_2^2$$
$$-\frac{1}{2\psi_1}(\varrho_1-\psi_1\hat{\varrho}_1)^2+\frac{\varrho_1}{2\psi_1}+\frac{\varrho_1}{4\sigma_1}+\bar{m}_1^2+\bar{m}_2^2$$
$$+z_3(\psi_1 z_2+z_4+\alpha_3-\vartheta_3-\dot{\chi}_3) \tag{39}$$

Here, let $\mathcal{L}_2=\psi_1 z_2-\dot{\chi}_3-\vartheta_3$. Furthermore, taking the following operation for $\mathcal{L}_2$

$$|\mathcal{L}_2|\le\varrho_2\beta_2(\varsigma_2) \tag{40}$$

where $\varrho_2=\max\{\psi_1,1\}$ and $\beta_2(\varsigma_2)=|z_2|+|\dot{\chi}_3+\vartheta_3|$ with $\varsigma_2=[z_2,\dot{\chi}_3,\vartheta_3]^T$. Furthermore, one can get

$$|z_3\mathcal{L}_2|\le|z_3|\varrho_2\beta_2(\varsigma_2)\le\sigma_2\varrho_2 z_3^2\beta_2^2(\varsigma_2)+\frac{\varrho_2}{4\sigma_2} \tag{41}$$

where σ_2 is a positive constant.

Invoking (41) into (39) yields

$$\dot{V}_3^*\le-(k_1-1)z_1^2-(\tau^{-1}-1)\sum_{i=1}^{2}\vartheta_i^2-\psi_1 k_2 z_2^2$$
$$-\frac{1}{2\psi_1}(\varrho_1-\psi_1\hat{\varrho}_1)^2+\frac{\varrho_1}{2\psi_1}+\bar{m}_1^2+\bar{m}_2^2$$
$$+z_3(z_4+\alpha_3+\sigma_2\varrho_2 z_3\beta_2^2(\varsigma_2))+\sum_{i=1}^{2}\frac{\varrho_i}{4\sigma_i} \tag{42}$$

Design the virtual control law α_3 as

$$\alpha_3=-k_3 z_3-\sigma_2\hat{\varrho}_2 z_3\beta_2^2(\varsigma_2) \tag{43}$$

with the adaptive law

$$\dot{\hat{\varrho}}_2=\sigma_2\hat{\varrho}_2 z_3^2\beta_2^2(\varsigma_2)-\mu_2\hat{\varrho}_2 \tag{44}$$

where k_3 and μ_2 are the design constants.

Consider the following Lyapunov function candidate

$$V_3=V_3^*+\frac{1}{2}(\varrho_2-\hat{\varrho}_2)^2+\frac{1}{2}\vartheta_3^2 \tag{45}$$

Taking the time-derivative of V_3, and substituting (43)-(45) into (42) yield

$$\dot{V}_3\le-(k_1-1)z_1^2-(\tau^{-1}-1)\sum_{i=1}^{3}\vartheta_i^2-\psi_1 k_2 z_2^2$$
$$-\frac{\mu_1}{2\psi_1}(\varrho_1-\psi_1\hat{\varrho}_1)^2-\frac{\mu_2}{2}(\varrho_2-\hat{\varrho}_2)^2+z_3(z_4-k_3 z_3)$$
$$+\sum_{i=1}^{2}\frac{\varrho_i}{4\sigma_i}+\frac{\mu_1\varrho_1}{2\psi_1}+\frac{2\bar{m}_1^2+\bar{m}_2^2+\bar{m}_3^2}{4}+\frac{\mu_2\varrho_2}{2} \tag{46}$$

Step 4: According to (9) and (14), the time-derivative of z_4 is given by

$$\dot{z}_4=\psi_2\epsilon u_c+f_4(\bar{x}_4)-\dot{\chi}_4+d \tag{47}$$

From the Assumption 2, $f_4(\bar{x}_4)$ in (47) is an unknown function, which can not be used in the control law design. Here, the RBF NN $\xi_4^{*T}\Psi(\bar{x}_4)$ is applied to approximate $f_4(\bar{x}_4)$. Then, $f_4(\bar{x}_4)$ can be written as

$$f_4(\bar{x}_4)=\xi_4^{*T}\Psi(\bar{x}_4)+\varepsilon_4 \tag{48}$$

where ε_4 is the approximation error satisfying $|\varepsilon_4|\le\delta_4$ with $\delta_4>0$ being an unknown constant. Invoking (48) into (47), one obtains

$$\dot{z}_4=\psi_2\epsilon u_c+\xi_4^{*T}\Psi(\bar{x}_4)+\varepsilon_4-\dot{\chi}_4+d \tag{49}$$

Let $\mathcal{L}_3=\xi_4^{*T}\Psi(\bar{x}_4)+\varepsilon_4-\dot{\chi}_4-z_3+d$. Since $\mathcal{L}_3$ includes the unknown term $\xi_4^{*T}\Psi(\bar{x}_4)+\varepsilon_4+d$, it can not be used. Here, taking the following operation for $\mathcal{L}_3$ yields

$$|\mathcal{L}_3|\le|\xi_4^{*T}\Psi(\bar{x}_4)|+|\varepsilon_4+d|+|\dot{\chi}_4+z_3|$$
$$\le\varrho_3\beta_3(\varsigma_3) \tag{50}$$

where $\varrho_3=\max\{||\xi_4||,|\varepsilon_4+d|,1\}$ and $\beta_3(\varsigma_3)=||\Psi(\bar{x}_4)||+|\dot{\chi}_4+z_3|+1$ with $\varsigma_3=[\bar{x}_4^T,\dot{\chi}_4,z_3]^T$.

Synthesizing (49) and (50) yields

$$z_4\dot{z}_4\le z_4\psi_2\epsilon u_c+|z_4|\varrho_3\beta_3(\varsigma_3)+z_4 z_3$$
$$\le z_4\psi_2\epsilon u_c+\varrho_3\sigma_3 z_4^2\beta_3^2(\varsigma_3)+z_4 z_3+\frac{\varrho_3}{4\sigma_3} \tag{51}$$

Design the following control input $\widehat{u}_c$

$$\widehat{u}_c=-k_4 z_4-\hat{\varrho}_3\sigma_3 z_4\beta_3^2(\varsigma_3) \tag{52}$$

with the adaptive law

$$\dot{\hat{\varrho}}_3 = \sigma_3 z_4^2 \beta_3^2(\varsigma_3) - \mu_3 \hat{\varrho}_3 \tag{53}$$

and the event triggering mechanism

$$\begin{aligned} u_c(t) &= \widehat{u}_c(t), t \in [t_J, t_{J+1}); \\ t_{J+1} &= \inf\left\{t \in R \mid (|s| \geq \epsilon_s u_0) \cup (|z_1| \geq \epsilon_z u_0)\right\} \end{aligned} \tag{54}$$

where k_4, σ_3, μ_3, ϵ_s and ϵ_z are design constants, $s = u_c - \widehat{u}_c$ is the measuring error and $u_0 = \frac{a}{\int_{t_0}^{t} |s(\tau)| d(\tau) + a_1}$ with a and a_1 being positive constants.

Remark 5: From (54), one can get that the control command generated by the control law (52) is transferred to the actuator when the event is trigged, and meanwhile the actuator responses the control command. In this case, within the the holding phase, i.e., for $\forall t \in [t_J, t_{J+1})$, the actuator only executes the control command $\widehat{u}_c(t)$ at $t = t_J$. Therefore, compared with the continuous time control scheme, our proposed ETC scheme can reduce the response frequency of control command $\widehat{u}_c(t)$ such that the mechanical wear can also be reduced.

Considering the following Lyapunov function candidate

$$V_4 = V_3 + \frac{1}{2} z_4^2 + \frac{1}{2\psi_\epsilon} (\varrho_3 - \psi_\epsilon \hat{\varrho}_3)^2 \tag{55}$$

Taking the time derivative of V_4 and using (51)-(53) yield

$$\begin{aligned} \dot{V}_4 \leq \dot{V}_3 + z_4 \psi_2 \epsilon (u_c - \widehat{u}_c) - \psi_\epsilon k_4^2 + z_4 z_3 \\ + (\varrho_3 - \psi_\epsilon \hat{\varrho}_3) \mu_3 \hat{\varrho}_3 + \frac{\varrho_3}{4\sigma_3} \end{aligned} \tag{56}$$

According to the event triggering mechanism (54), one can get $u_c - \widehat{u}_c$ is bounded, i.e., $|s| \leq b$ with b is a constant. And then, the term $z_4 \psi_2 \epsilon (u_c - \widehat{u}_c)$ can be rewritten as

$$z_4 \psi_2 \epsilon (u_c - \widehat{u}_c) \leq \frac{1}{2} \psi_\epsilon z_4^2 + \frac{\psi_\epsilon b^2}{2} \tag{57}$$

Using (46) and (57), (55) can be written as

$$\begin{aligned} \dot{V}_4 \leq & -(k_1 - 1) z_1^2 - (\tau^{-1} - 1) \sum_{i=1}^{3} \vartheta_i^2 - \psi_1 k_2 z_2^2 \\ & - \frac{\mu_1}{2\psi_1} (\varrho_1 - \psi_1 \hat{\varrho}_1)^2 - \frac{\mu_2}{2} (\varrho_2 - \hat{\varrho}_2)^2 - k_3 z_3^2 \\ & + \sum_{i=1}^{3} \frac{\varrho_i}{4\sigma_i} + \frac{\mu_1 \varrho_1}{2\psi_1} + \frac{2\bar{m}_1^2 + \bar{m}_2^2 + \bar{m}_3^2}{4} + \frac{\mu_2 \varrho_2}{2} \\ & - \frac{1}{2} \psi_\epsilon k_4^2 - \frac{\mu_3}{2\psi_\epsilon} (\varrho_3 - \psi_\epsilon \hat{\varrho}_3)^2 + \frac{\mu_3}{2\psi_\epsilon} \\ \leq & -\zeta V_4 + \rho \end{aligned} \tag{58}$$

where $\zeta = \min\{2(k_1 - 1), 2\psi_1 k_2, 2k_3, \psi_\epsilon, 2\tau(1-\tau), \mu_1, \mu_2, \mu_3\}$ and $\rho = \sum_{i=1}^{3} \frac{\varrho_i}{4\sigma_i} + \frac{\mu_1 \varrho_1}{2\psi_1} + \frac{2\bar{m}_1^2 + \bar{m}_2^2 + \bar{m}_3^2}{4} + \frac{\mu_2 \varrho_2}{2} + \frac{\mu_3}{2\psi_\epsilon}$

B. STABILITY ANALYSIS

The above design and analysis is given by the following theorem.

Theorem 1: Considering the closed-loop control system consisting of the mathematical model of single-link FJR (1)-(2) subject to dynamic uncertainties and input saturation, if the assumptions 1-2 are satisfied, the adaptive control law (52) with the virtual control laws (18), (28) and (43), the adaptive laws (19), (29) and (44) and (53), and the event triggering mechanism (54) can ensure the following statements to be held.

- All signals in the closed-loop control system are bounded.
- The Zeno behavior caused by the event triggering mechanism can be avoided.

Proof: 1) *The boundedness of all signals in the closed-loop control system.* Solving (58) yields

$$V_4 \leq \left(V_4(0) + \frac{\rho}{\zeta}\right) \exp(-\zeta t) + \frac{\rho}{\zeta} \tag{59}$$

Here, $V_4(0)$ is the initial value of V_4. From (59), $V_4 = \frac{\rho}{\zeta}$ as $t \to \infty$, which shows that V_4 is bounded. Furthermore, according to (19), (30), (45) and (55), the boundedness of z_j ($j = 1, 2, 3, 4$), $\hat{\varrho}_i$ ($i = 1, 2, 3$) and ϑ_i can be determined. According to assumption 2 and (13), x_1 is bounded, and meanwhile the boundedness of α_1 can be determined. In addition, from (7) and the boundedness of ϑ_1, one can get that χ_2 is boundedness. Similarly, one can obtain that x_2, x_3, x_4, α_2, α_3, ϑ_2, ϑ_3 χ_3 and χ_4 are also bounded; furthermore, the boundedness of $\hat{\varrho}_2$ and $\hat{\varrho}_3$ can also be determined. From (50) and the boundedness of z_4, z_3, $\hat{\varrho}_3$ and χ_4, one can get the boundedness of $\widehat{u}_c$. Therefore, all signals in the closed-loop control system are bounded.

2) *Zeno behavior avoidance*. According to the event triggering mechanism (54), in the holding phase of $\widehat{u}_c$, i.e., $t \in [t_j, t_{j+1})$, the actual control command u_c is a constant, which implies that there is a variance between u_c and $\widehat{u}_c$, i.e., the control measurement error $s = u_c - \widehat{u}_c$. Taking the time derivative of $|s|$ yields

$$\frac{d|s|}{dt} = \operatorname{sgn}(s)\dot{s} \leq |\dot{\widehat{u}}_c| \tag{60}$$

According to (13)-(15), (50), (52) and (53), one has

$$\begin{aligned} \dot{\widehat{u}}_c = & \frac{\partial \widehat{u}_c}{\partial z_4} \dot{z}_4 + \frac{\partial \widehat{u}_c}{\partial \hat{\varrho}_3} \dot{\hat{\varrho}}_3 + \frac{\partial \widehat{u}_c}{\partial \varsigma_2} \frac{\partial \varsigma_2}{\bar{x}_4} \dot{\bar{x}}_4 \\ & + \frac{\partial \widehat{u}_c}{\partial \varsigma_2} \frac{\partial \varsigma_2}{z_3} \dot{z}_3 + \frac{\partial \widehat{u}_c}{\partial \varsigma_2} \frac{\partial \varsigma_2}{\dot{\chi}_4} \ddot{\chi}_4 \end{aligned} \tag{61}$$

According to the boundedness of z_4, $\dot{\chi}_4$, x_4 and u_c, one can get that $\dot{z}_4$ is bounded from (49). From (53), it can be found that $\dot{\hat{\varrho}}_3$ is bounded. In addition, from the boundedness of z_3 and $\dot{\chi}_4$, one can get that $\dot{z}_3$ and $\ddot{\chi}_4$ are bounded from (41), (15) and $\vartheta_4 = \chi_4 - \alpha_3$. Therefore, $\dot{\widehat{u}}_c$ is bounded by $\bar{u}$. For $t \in [t_J, t_{J+1})$, taking the fact of $u_c(t_J) = 0$ and $\lim_{t \to t_{J+1}} \min s(t) = \bar{s}$ being into account, one can get that the lower bound $\underline{t}$ of inter-execution interval $\check{t} = t_{J+1} - t_J$ meets

$\check{t} \geq \underline{t} \geq \bar{s}/\bar{u}_c$, which indicates that the Zeno behavior caused by the event triggering mechanism is avoided in this work.

IV. SIMULATION RESULTS

In this section, a single-link FJR system is employed to illuminate the effectiveness of the proposed control scheme. In the simulation, the dynamic parameters of single-link FJR are given by $\mathcal{M} = 0.25\ kg$, $\mathcal{L} = 1m$, $g = 9.8m/s^2$, $\mathcal{K} = 2N \cdot m/rad$, $\mathcal{J} = 0.001$, $\mathcal{B} = 0.6$ and $\mathcal{F}(\dot{q}) = 0.1\cos(\dot{q})$. The reference trajectory is given by $y_d = 0.5(\sin t + \sin(0.5t))$.

In the simulation, the design constants of the control law are set as $k_1 = 5$, $k_2 = 35$, $k_3 = 20$, $k_4 = 3$, $\tau = 0.25$, $\sigma_1 = 2$, $\mu_1 = 0.2$, $\sigma_2 = 1$, $\mu_2 = 0.5$, $\sigma_3 = 5$,$\mu 3 = 2$, $\varepsilon_z = \varepsilon_s = 1$, $a = 0.35$ and $a_1 = 0.35$, $t_0 = 0.2$. The maximum $u_{\max}$ of the control input u is $u_{\max} = 2.2$. The initial conditions are given by $x_1(0) = x_2(0) = x_3(0) = x_4(0) = 0$ and $\varrho_i(0) = 0$, $(i = 1, 2, 3)$. The RBF NNs for $f_2(\bar{\boldsymbol{x}}_2)$ and $f_4(\bar{\boldsymbol{x}}_4)$ contain 20 nodes with centers evenly spaced in the range $[-2, 2]\times[-2, 2]$ with $\omega_i = 1$.

To indicate the effective of the proposed ETABTC scheme, a simulation comparison with the time-triggering control scheme is carried out, and the time-triggering control law u_c replaces the event-triggering control law, i.e., $u_c = \widehat{u}_c$.

Simulation results under the proposed control laws u_{etc} and u_c as shown in Figs. 1-5. Fig. 1 shows the tracking control performance under two control laws, which demonstrates that both two control laws can force the link position q to track the reference trajectory y_d with satisfying performance. The result in Fig. 2 demonstrate that the tracking control accuracy of the continuous time control scheme is slightly better than the proposed ETABTC scheme, which indicates that the proposed ETABTC scheme has control energy loss due to the event triggering mechanism (54). Fig. 3 presents the control inputs under the continuous time control scheme and proposed ETABTC scheme, from which the actual control input u is bounded and reasonable. In addition, it can be observed from Fig. 3 that the actual control input u satisfies $u \leq u_m$,

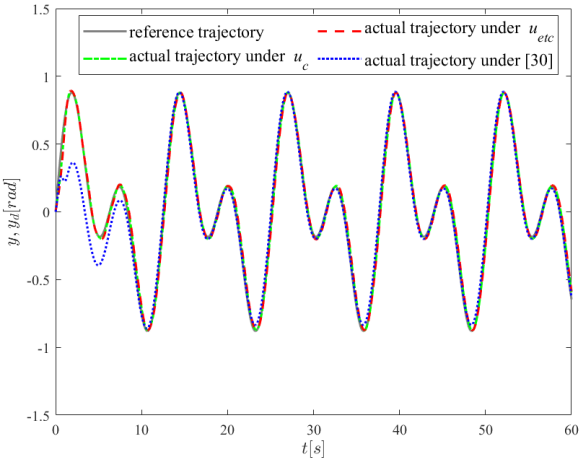

FIGURE 1. Trajectories of the link position q and the reference trajectory y_d.

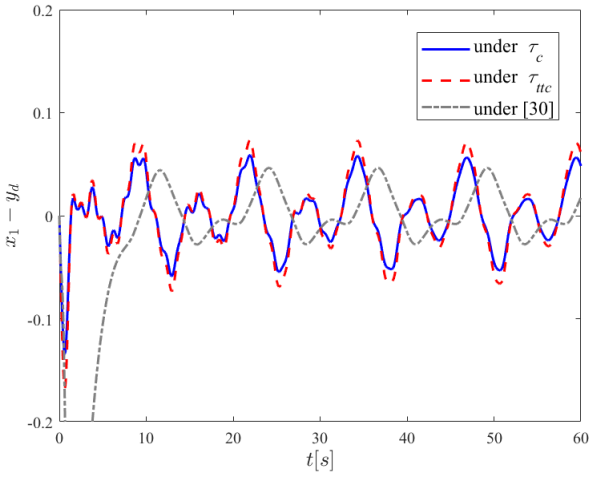

FIGURE 2. The tracking error z_1.

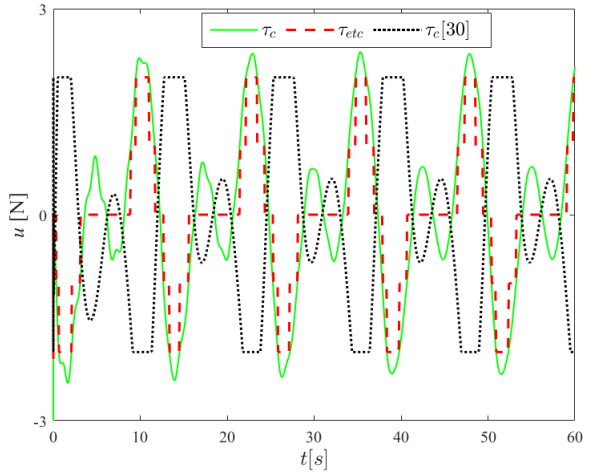

FIGURE 3. The control input u.

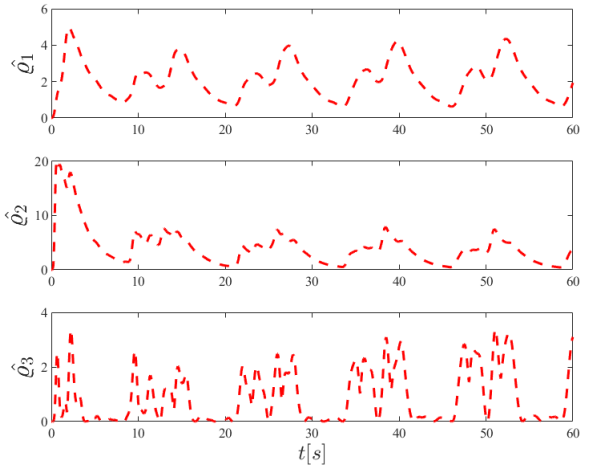

FIGURE 4. The estimations of ϱ_i, $i = 1, 2, 3$.

which indicates the effectiveness of the continuous time control scheme and proposed ETABTC scheme. Fig. 4 presents the curve of $\hat{\varrho}_i$ $(i = 1, 2, 3)$, which shows that the estimation

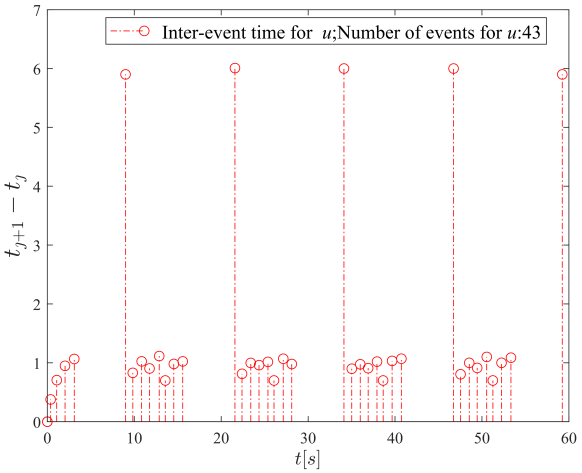

FIGURE 5. Triggering instants and triggering time.

of ϱ_i is bounded. Fig. 5 draws the triggering instants and triggering times, from which it can be clearly found that the control command u_{etc} is not transmitted indefinitely over a short period of time. Under the proposed ETABTC scheme, the actuator responses to the control commands generated by control law (52) 41 times. These results demonstrate that all signals in the closed-loop control system of FJR are bounded, as proven in Theorem 1. Therefore, the proposed ETABTC scheme is effective.

Furthermore, to clarify the superiority of the proposed ETABTC scheme, a comparison simulation is carried out between the proposed ETABTC scheme and the scheme proposed in [30]. All design parameters of the scheme proposed in [30] are taken the same as the work [30], and the initial conditions are identical to our control scheme. The simulation results are shown in Figs. 1-3, from which it can found that the scheme in [30] can also force the the link position q to track the reference trajectory y_d as the same as our proposed ETABTC scheme. Although the control accuracy shown in Fig.3 under the control scheme in [30] is superior to that one of ETABTC scheme, the control scheme in [30] requires the norm parts of plant. In contrast, our proposed ETABTC scheme is more practical since no knowledge of plant is required in the control design.

V. CONCLUSION

This work develops an event-triggered adaptive neural tracking control solution for FJR systems under unknown dynamics and input saturation. A smooth function is introduced to handle the input saturation nonlinearity, and adaptive neural reconstruction techniques is used to compensate the unknown dynamics online. The DSC and single-parameter-learning techniques are used to handle the ''explosion of complexity'' and computational burden issues, respectively. In the control design, an event-triggered mechanism is established between the control law and actuator. Finally, an event-triggered adaptive neural tracking control scheme is proposed. The stability of the closed-loop system of FJR systems' tracking was proof by Lyapunov theory. Simulation results validate the effectiveness and superiority of the proposed control scheme.

In the future, the work will be extended to a more general system, such as the time-varying control gain, multiple-input-multiple-output, non-affine system, etc. In addition, the further work is to reduce the response frequency of the actuator by one step.

REFERENCES

[1] S. Ozgoli and H. D. Taghirad, "A survey on the control of flexible joint robots," *Asian J. Control*, vol. 8, no. 4, pp. 332–344, 2006.
[2] H. Wang, Y. Zhang, Z. Zhao, X. Tang, J. Yang, and I.-M. Chen, "Finite-time disturbance observer-based trajectory tracking control for flexible-joint robots," *Nonlinear Dyn.*, vol. 106, no. 1, pp. 459–471, Sep. 2021.
[3] A. Ailon, R. Lozano, and M. I. Gil, "Iterative regulation of an electrically driven flexible-joint robot with model uncertainty," *IEEE Trans. Robot. Autom.*, vol. 16, no. 6, pp. 863–870, Dec. 2000.
[4] M. Kim, F. Beck, C. Ott, and A. Albu-Schäffer, "Model-free friction observers for flexible joint robots with torque measurements," *IEEE Trans. Robot.*, vol. 35, no. 6, pp. 1508–1515, Dec. 2019.
[5] X. Liu, C. Yang, Z. Chen, M. Wang, and C. Y. Su, "Neuro-adaptive observer based control of flexible joint robot," *Neurocomputing*, vol. 275, pp. 73–82, Jan. 2018.
[6] P. Tomei, "An observer for flexible joint robots," *IEEE Trans. Autom. Control*, vol. 35, no. 6, pp. 739–743, Jun. 1990.
[7] H. A. Malki, D. Misir, D. Feigenspan, and G. Chen, "Fuzzy PID control of a flexible-joint robot arm with uncertainties from time-varying loads," *IEEE Trans. Control Syst. Techn.*, vol. 5, no. 3, pp. 371–378, May 1997.
[8] A. de Luca, B. Siciliano, and L. Zollo, "PD control with on-line gravity compensation for robots with elastic joints: Theory and experiments," *Automatica*, vol. 41, no. 10, pp. 1809–1819, Oct. 2005.
[9] M. J. Kim and W. K. Chung, "Disturbance-observer-based PD control of flexible joint robots for asymptotic convergence," *IEEE Trans. Robot.*, vol. 31, no. 6, pp. 1508–1516, Dec. 2015.
[10] A.-C. Huang and Y.-C. Chen, "Adaptive sliding control for single-link flexible-joint robot with mismatched uncertainties," *IEEE Trans. Control Syst. Technol.*, vol. 12, no. 5, pp. 770–775, Sep. 2004.
[11] K. Melhem and W. Wang, "Global output tracking control of flexible joint robots via factorization of the manipulator mass matrix," *IEEE Trans. Robot.*, vol. 25, no. 2, pp. 428–437, Apr. 2009.
[12] M. Ramírez-Neria, G. Ochoa-Ortega, N. Lozada-Castillo, M. A. Trujano-Cabrera, J. P. Campos-López, and A. Luviano-Juárez, "On the robust trajectory tracking task for flexible-joint robotic arm with unmodeled dynamics," *IEEE Access*, vol. 4, pp. 7816–7827, 2016.
[13] J. R. Forbes and C. J. Damaren, "Design of optimal strictly positive real controllers using numerical optimization for the control of flexible robotic systems," *J. Franklin Inst.*, vol. 348, no. 8, pp. 2191–2215, Oct. 2011.
[14] J. Kim and E. A. Croft, "Full-state tracking control for flexible joint robots with singular perturbation techniques," *IEEE Trans. Control Syst. Technol.*, vol. 27, no. 1, pp. 63–73, Jan. 2019.
[15] J. S. Bang, H. Shim, S. K. Park, and J. H. Se, "Robust tracking and vibration suppression for a two-inertia system by combining backstepping approach with disturbance observer," *IEEE Trans. Ind. Electron.*, vol. 57, no. 9, pp. 3197–3206, Sep. 2010.
[16] M. S. Kim and J. S. Lee, "Adaptive tracking control of flexible-joint manipulators without overparametrization," *J. Robot. Syst.*, vol. 21, no. 7, pp. 369–379, Jul. 2004.
[17] W. Chang, Y. Li, and S. Tong, "Adaptive fuzzy backstepping tracking control for flexible robotic manipulator," *IEEE/CAA J. Autom. Sinica*, vol. 8, no. 12, pp. 1923–1930, Dec. 2021.
[18] M. Krstić, P. V. Kokotovic, and I. Kanellakopoulos, *Nonlinear and Adaptive Control Design*. Hoboken, NJ, USA: Wiley, 1995.
[19] D. Swaroop, J. K. Hedrick, P. P. Yip, and J. C. Gerdes, "Dynamic surface control for a class of nonlinear systems," *IEEE Trans. Autom. Control*, vol. 45, no. 10, pp. 1893–1899, Oct. 2000.
[20] S. J. Yoo, J. B. Park, and Y. H. Choi, "Adaptive dynamic surface control of flexible-joint robots using self-recurrent wavelet neural networks," *IEEE Trans. Syst., Man, Cybern. B, Cybern.*, vol. 36, no. 6, pp. 1342–1355, Dec. 2006.

[21] Y. Li, S. Tong, and T. Li, "Fuzzy adaptive dynamic surface control for a single-link flexible-joint robot," *Nonlinear Dyn.*, vol. 70, no. 3, pp. 2035–2048, Sep. 2012.
[22] S. J. Yoo, J. B. Park, and Y. H. Choi, "Output feedback dynamic surface control of flexible-joint robots," *Int. J. Control Automat. Syst.*, vol. 6, no. 2, pp. 223–233, Apr. 2008.
[23] K. Rsetam, Z. Cao, and Z. Man, "Cascaded-extended-state-observer-based sliding-mode control for underactuated flexible joint robot," *IEEE Trans. Ind. Electron.*, vol. 67, no. 12, pp. 10822–10832, Dec. 2020.
[24] S. E. Talole, J. P. Kolhe, and S. B. Phadke, "Extended-state-observer-based control of flexible-joint system with experimental validation," *IEEE Trans. Ind. Electron.*, vol. 57, no. 4, pp. 1411–1419, Apr. 2010.
[25] A. Saleki and M. M. Fateh, "Model-free control of electrically driven robot manipulators using an extended state observer," *Comput. Electr. Eng.*, vol. 87, Oct. 2020, Art. no. 106768.
[26] M. Jin, J. Lee, and N. G. Tsagarakis, "Model-free robust adaptive control of humanoid robots with flexible joints," *IEEE Trans. Ind. Electron.*, vol. 64, no. 2, pp. 1706–1715, Feb. 2017.
[27] J. Lee, P. H. Chang, and M. Jin, "Adaptive integral sliding mode control with time-delay estimation for robot manipulators," *IEEE Trans. Ind. Electron.*, vol. 64, no. 8, pp. 6796–6804, Aug. 2017.
[28] L. Ma, N. Xu, X. Zhao, G. Zong, and X. Huo, "Small-gain technique-based adaptive neural output-feedback fault-tolerant control of switched nonlinear systems with unmodeled dynamics," *IEEE Trans. Syst., Man, Cybern., Syst.*, vol. 51, no. 11, pp. 7051–7062, Nov. 2021.
[29] Z. Chen, M. Wang, and Y. Zou, "Dynamic learning from adaptive neural control for flexible joint robot with tracking error constraints using high-gain observer," *Syst. Sci. Control Eng.*, vol. 6, no. 3, pp. 177–190, Nov. 2018.
[30] S. Ling, H. Wang, and P. X. Liu, "Adaptive fuzzy tracking control of flexible-joint robots based on command filtering," *IEEE Trans. Ind. Electron.*, vol. 67, no. 5, pp. 4046–4055, May 2020.
[31] S. Diao, W. Sun, S.-F. Su, and J. Xia, "Adaptive fuzzy event-triggered control for single-link flexible-joint robots with actuator failures," *IEEE Trans. Cybern.*, early access, Jan. 27, 2021, doi: 10.1109/TCYB.2021.3049536.
[32] S. J. Yoo, J. B. Park, and Y. H. Choi, "Adaptive output feedback control of flexible-joint robots using neural networks: Dynamic surface design approach," *IEEE Trans. Neural Netw.*, vol. 19, no. 10, pp. 1712–1726, Oct. 2008.
[33] Z. Miao and Y. Wang, "Robust dynamic surface control of flexible joint robots using recurrent neural networks," *J. Control Theory Appl.*, vol. 11, no. 2, pp. 222–229, May 2013.
[34] G. Zhu, J. Du, and Y. Kao, "Robust adaptive neural trajectory tracking control of surface vessels under input and output constraints," *J. Franklin Inst.*, vol. 357, no. 13, pp. 8591–8610, Sep. 2020.
[35] G. Zhu, Y. Ma, Z. Li, R. Malekian, and M. Sotelo, "Adaptive neural output feedback control for MSVs with predefined performance," *IEEE Trans. Veh. Technol.*, vol. 70, no. 4, pp. 2994–3006, Apr. 2021.
[36] S. Ling, H. Wang, and P. X. Liu, "Adaptive fuzzy dynamic surface control of flexible-joint robot systems with input saturation," *IEEE/CAA J. Autom. Sinica*, vol. 6, no. 1, pp. 97–107, Jan. 2019.
[37] M. M. Rayguru, S. Roy, and I. N. Kar, "Time-scale redesign-based saturated controller synthesis for a class of MIMO nonlinear systems," *IEEE Trans. Syst., Man, Cybern., Syst.*, vol. 51, no. 8, pp. 4681–4692, Aug. 2021.
[38] B. Niu and H. Zhang, "Linear parameter-varying modeling for gain-scheduling robust control synthesis of flexible joint industrial robot," *Proc. Eng.*, vol. 41, pp. 838–845, Jan. 2012.
[39] J. Huang, C. Wen, W. Wang, and Y.-D. Song, "Global stable tracking control of underactuated ships with input saturation," *Syst. Control Lett.*, vol. 85, pp. 1–7, Nov. 2015.
[40] G. Zhu, J. Du, and Y. Kao, "Command filtered robust adaptive NN control for a class of uncertain strict-feedback nonlinear systems under input saturation," *J. Franklin Inst.*, vol. 355, no. 15, pp. 7548–7569, Oct. 2018.
[41] X. Hu, X. Wei, J. Han, and X. Zhu, "Adaptive disturbance estimation and cancelation for ships under thruster saturation," *Int. J. Robust Nonlinear Control*, vol. 30, no. 13, pp. 5004–5020, Sep. 2020.
[42] G. Zhu, Y. Ma, and S. Hu, "Single-parameter-learning-based finite-time tracking control of underactuated MSVs under input saturation," *Control Eng. Pract.*, vol. 105, Dec. 2020, Art. no. 104652.
[43] S. Ding, J. Peng, H. Zhang, and Y. Wang, "Neural network-based adaptive hybrid impedance control for electrically driven flexible-joint robotic manipulators with input saturation," *Neurocomputing*, vol. 458, pp. 99–111, Oct. 2021.
[44] W. Qi, G. Zong, and W. X. Zheng, "Adaptive event-triggered SMC for stochastic switching systems with semi-Markov process and application to boost converter circuit model," *IEEE Trans. Circuits Syst. I, Reg. Papers*, vol. 68, no. 2, pp. 786–796, Feb. 2021.
[45] W. Qi, Y. Hou, G. Zong, and C. K. Ahn, "Finite-time event-triggered control for semi-Markovian switching cyber-physical systems with FDI attacks and applications," *IEEE Trans. Circuits Syst. I, Reg. Papers*, vol. 68, no. 6, pp. 2665–2674, Jun. 2021.
[46] M. Mazo, Jr., A. Anta, and P. Tabuada, "An ISS self-triggered implementation of linear controllers," *Automatica*, vol. 46, no. 8, pp. 1310–1314, Aug. 2010.
[47] S. Li, C. K. Ahn, J. Guo, and Z. Xiang, "Neural-network approximation-based adaptive periodic event-triggered output-feedback control of switched nonlinear systems," *IEEE Trans. Cybern.*, vol. 51, no. 8, pp. 4011–4020, Aug. 2021.
[48] J. Zhang, S. Li, C. K. Ahn, and Z. Xiang, "Decentralized event-triggered adaptive fuzzy control for nonlinear switched large-scale systems with input delay via command-filtered backstepping," *IEEE Trans. Fuzzy Syst.*, early access, Mar. 17, 2021, doi: 10.1109/TFUZZ.2021.3066297.
[49] G. Zhu, Y. Ma, Z. Li, R. Malekian, and M. Sotelo, "Event-triggered adaptive neural fault-tolerant control of underactuated MSVs with input saturation," *IEEE Trans. Intell. Transp. Syst.*, early access, Mar. 24, 2021, doi: 10.1109/TITS.2021.3066461.
[50] S. Diao, W. Sun, S.-F. Su, and J. Xia, "Adaptive fuzzy event-triggered control for single-link flexible-joint robots with actuator failures," *IEEE Trans. Cybern.*, early access, Jan. 27, 2021, doi: 10.1109/TCYB.2021.3049536.
[51] T. Cheng, B. Niu, G. Zhang, Z. Wang, and P. Duan, "Event-triggered-based adaptive command-filtered asymptotic tracking control for flexible robotic manipulators," *Nonlinear Dyn.*, vol. 105, no. 2, pp. 1543–1557, Jul. 2021.
[52] J. Zhang, B. Niu, D. Wang, H. Wang, P. Zhao, and G. Zong, "Time-/event-triggered adaptive neural asymptotic tracking control for nonlinear systems with full-state constraints and application to a single-link robot," *IEEE Trans. Neural Netw. Learn. Syst.*, early access, Jun. 2, 2021, doi: 10.1109/TNNLS.2021.3082994.

XINGLEI XU received the B.S. degree from Wenzhou University, China, in 2006, and the M.S. degree from Tongji University, China, in 2012. He is currently with the Department of Information Technology, Wenzhou Polytechnic, China. His research interests include artificial intelligence and machine vision.

SHIWEI XU received the B.S. degree from the Zhejiang University of Technology, China, in 2009, and the M.S. degree from Zhejiang University, China, in 2012. He is currently with the Department of Information Technology, Wenzhou Polytechnic, China. His research interests include computer vision algorithm design and its application in intelligent manufacturing.